Int. J. Solids Structures Vol. 23, No 2, pp. 239–252, 1987
Printed in Great Britain

0020-7683/87 $3.00+.00
Pergamon Journals Ltd.

STRESSES IN THE REGION OF ROUNDED CORNERS

J. P. BENTHEM
Laboratory of Engineering Mechanics, Mekelweg 2, Delft, The Netherlands

(*Received* 23 *September* 1985; *in revised form* 28 *February* 1986)

Abstract—The mode I state of stress around a crack front, i.e. in a "wedge" of angle $\alpha = 2\pi$, is well defined by the stress intensity factor K_I. The stress $\sigma_y = K_I/\sqrt{(2\pi r)}$ becomes infinite at the vertex $r = 0$. It is known that if the sharp crack is rounded by a radius ρ, small with respect to crack length and other dimensions, the maximum value for the stress σ_y only becomes $\sigma_y = 2K_I/\sqrt{(\pi\rho)}$. By numerical solution of integral equations corresponding results are given for wedges of arbitrary angles $\pi < \alpha < 2\pi$ in state of modes I, II and III. The method was verified by comparison with the exact solution for mode III. Such an exact solution is not possible for modes I and II.

1. INTRODUCTION

Williams [1] determined two-dimensional stress singularities of regions which locally can be considered as wedges. Such stress singularities have the shape

$$\sigma = cr^{\lambda} f[\lambda, \theta] \tag{1}$$

where r and θ are polar coordinates with the origin in the corner of the wedge. The exponent λ determines the *character* of the singularity and the participation factor c determines its *strength*.

Williams' characteristic equation for the exponents λ (eigenvalues) for the wedge of angle α in plane strain (also plane stress) with traction-free sides is

$$\sin^2\{(\lambda + 1)\alpha\} - (\lambda + 1)^2 \sin^2\alpha = 0. \tag{2}$$

In order that the strain energy in the neighbourhood of the corner ($r \to 0$) remains integrable to a finite amount, λ must be greater than -1.† There is an infinite enumerable number of roots for the eigenvalue λ and stress fields belonging to these roots (eigenstates). All these eigenstates will generally be present in the wedge-shaped region, but the field belonging to the λ most close to -1 will prevail over all the other fields if $r \to 0$. All two-dimensional states of stress in a traction-free wedge-shaped region are only the sum of all the eigenstates (with $\lambda > -1$), because these eigenstates form a complete set. Such a completeness was already assumed for a long time, the rigorous proof was given in 1979[2].

Wedge-shaped regions in a symmetrical state of plane strain or plane stress are said occurring in mode I, in an antimetrical state in mode II and in anti-plane (torsion-like) state of stress in mode III (Fig. 1). For the latter state of stress a simpler characteristic equation is valid

$$\sin\{(\lambda + 1)\alpha\} = 0. \tag{3}$$

For the wedge angle $\alpha = 2\pi$ eqn (2) has double roots (> -1), $\lambda = -\frac{1}{2}, 0, \frac{1}{2}, 1, \frac{3}{2}, 2, \ldots$ and to each root belongs a symmetrical and an antimetrical eigenstate. Equation (3) for $\alpha = 2\pi$ has the same roots, but only single. To the three roots $\lambda = -\frac{1}{2}$ of eqns (2) and (3) together belong the well-known states of stress (eigenstates) with an inverse square-root stress singularity. In fracture mechanics the participation of these eigenstates is noted by means of the stress-intensity factors K_I, K_{II} and K_{III} for modes I, II and III, respectively. Today many computational techniques exist to compute stress-intensity factors in different configurations.

† In the present investigation only real roots λ need to be considered.

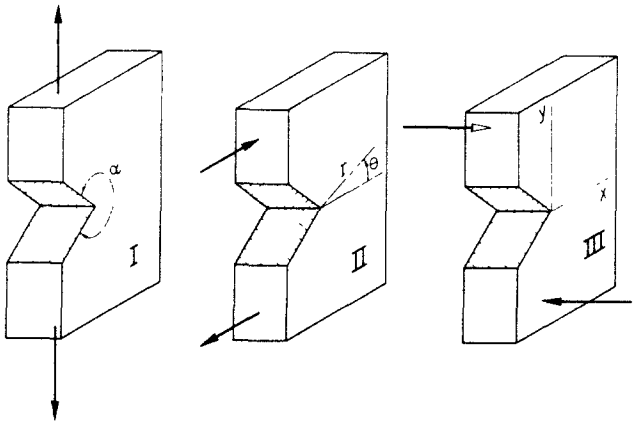

Fig. 1. Wedge-shaped region in modes I, II and III.

It should be emphasized that linear elasticity theory endures the infinite stresses at a sharp corner as long as the integrated strain energy remains finite. Of course the infinite stresses disappear if the sharp crack front is rounded by a radius ρ even only small compared with crack length and other dimensions of the overall configuration. From dimensional reasoning it may already be concluded that in the neighbourhood of the crack front rounded by a small radius ρ the stresses as function of dimensionless polar coordinates r/ρ, θ are proportional to $1/\sqrt{\rho}$. This means that once such a stress field is known for a small rounding radius, the stress fields for all other small rounding radii are also known. Such a stress field may be derived from the stress field in the region of the non-rounded crack tip and the latter field is determined by the stress-intensity factor K_I (or K_{II}, K_{III}). Thus determination of the stress-intensity factors may lead to the knowledge of the stresses in the rounded region. The main results for mode I (and III) are already known and use of these results is recommended in Sections 2.2 and 3.1 in Ref. [3] and on p. 17 in Ref. [4].

Likewise if a sharp corner of wedge angle $\pi < \alpha < 2\pi$ in which a state of stress, eqn (1), with an exponent $0 > \lambda > -\frac{1}{2}$ dominates is rounded by a small radius ρ, the stresses are proportional to ρ^{λ}. This fact is already recognized by Erdogan[5, Section 6]. Again this stress field can be computed for an arbitrary but small radius ρ from a known participation factor c (i.e. a generalization of the stress-intensity factor) of the sharp corner. Though the dominant eigenstates of the sharp corner are well known through Refs [1,2] and expressible in simple geometrical functions, the computation of the field of the rounded corner is not at all elementary and cannot lead to solutions in closed form for modes I and II, $\alpha < 2\pi$.

The purpose of this paper is to deliver the stress fields in the neighbourhood of corners rounded by a small radius if only the participation factor of the dominant eigenstate of the non-rounded sharp corner is computed. For the latter computation there are some numerical methods by means of well-proportioned finite elements[6–8]. Using finite elements at a corner with a small rounding radius ρ, however, may lead to ill-proportioned finite elements or to a large number of them.

2. THE TWO-DIMENSIONAL COMPLEX STRESS FUNCTIONS

2.1. *Plane strain and stress*

The Cartesian coordinates are x, y and $z = x + iy$. The stress components are σ_x, σ_y, τ. The complex stress functions are[9, p. 114]

$$\phi[z] \quad \text{and} \quad \psi[z] \tag{4}$$

and the stresses

$$\sigma_x - i\tau = \phi'[z] + \overline{\phi'[z]} - \bar{z}\phi''[z] - \psi'[z] \tag{5}$$

$$\sigma_y + i\tau = \phi'[z] + \overline{\phi'[z]} + \bar{z}\phi''[z] + \psi'[z]. \tag{6}$$

If the x- and y-axes are rotated by an angle γ (anti-clockwise) the stresses are[9, p. 25]

$$\sigma_x - i\tau = \phi'[z] + \overline{\phi'[z]} - (\bar{z}\phi''[z] + \psi'[z])e^{2i\gamma} \tag{7}$$

$$\sigma_y + i\tau = \phi'[z] + \overline{\phi'[z]} + (\bar{z}\phi''[z] + \psi'[z])e^{2i\gamma}. \tag{8}$$

In case of plane strain the third normal stress is (ν is Poisson's ratio)

$$\sigma_3 = \nu(\sigma_x + \sigma_y) = 2\nu(\phi'[z] + \overline{\phi'[z]}). \tag{9}$$

Along a traction-free boundary the (integrated) boundary condition for the stress functions becomes[9, pp. 115(33.1), 145(41.4) or 409(101.1)]

$$\phi[t] + t\overline{\phi'[t]} + \overline{\psi[t]} = \text{constant} \tag{10}$$

and t takes the z-values on the boundary.

2.2. *Anti-plane stress*

The shear stresses are τ_x and τ_y. The complex stress function is[10, p. 116]

$$\phi[z] \tag{11}$$

and the stresses

$$\tau_x - i\tau_y = i\phi'[z]. \tag{12}$$

If the x- and y-axes are rotated by an angle γ (anti-clockwise)

$$\tau_x - i\tau_y = i\phi'[z]e^{i\gamma}. \tag{13}$$

Along a traction-free boundary the (integrated) boundary condition for the stress function becomes

$$\phi[t] + \overline{\phi[t]} = \text{constant}. \tag{14}$$

3. EXACT SOLUTIONS FOR WEDGE ANGLE $\alpha = 2\pi$

3.1. *Mode I*

The starting point of the consideration will be a semi-infinite crack which occurs along the negative x-axis. Stress functions (4) for the dominant eigenstates are

$$\phi[z] = \frac{K_I}{\sqrt{(2\pi)}} z^{1/2}, \qquad \psi[z] = \frac{1}{2}\frac{K_I}{\sqrt{(2\pi)}} z^{1/2} \tag{15}$$

where K_I is the stress-intensity factor. The stress σ_y along the positive x-axis is

$$\sigma_y = \frac{K_I}{\sqrt{(2\pi)}} x^{-1/2}. \tag{16}\dagger$$

† Some authors use another stress-intensity factor, $\sigma_y = (K_I/\sqrt{2})x^{-1/2}$.

The rounding of the crackfront is achieved by considering a new boundary in the neighbourhood of the negative x-axis. This boundary is the parabola

$$z = \frac{\rho}{2}(1 - i\eta)^2, \quad -\infty < \eta < \infty \left(\text{i.e. } x = \frac{\rho}{2} - \frac{y^2}{2\rho} \right) \tag{17}$$

which has its focus in $z = 0$, its top in $z = \rho/2$ and at its top a radius of curvature ρ. Along this new boundary the tractions belonging to eigenstates (15) must be removed. This is done by additional stress functions

$$\phi_a[z] = 0, \qquad \psi_a[z] = -\frac{K_I}{\sqrt{(2\pi)}} \rho z^{-1/2}. \tag{18}$$

By substitution of (17) into the sums of eqns (15) and (18) and the result into eqn (10) it is easily verified that indeed the tractions along the parabola are now zero. The maximum stress occurs at the top of the parabola

$$(\sigma_y)_{\max} = \frac{2K_I}{\sqrt{\pi}} \rho^{-1/2}. \tag{19}$$

A stress-rounding factor R_I is defined by the quotient of the coefficients of eqns (19) and (16)

$$R_I = 2\sqrt{2}. \tag{20}$$

From eqns (16), (19) and (20)

$$(\sigma_y)_{\max} = \frac{K_I}{\sqrt{(2\pi)}} R_I \rho^{-1/2}, \qquad (R_I = 2\sqrt{2}). \tag{21}$$

This result occurs in Refs [3, p. 404(5); 4, p. 1.7(7); 11, p. 564], all without proofs.

It can easily be seen from stress functions (17) and (18) that the stresses expressed as functions of a dimensionless coordinate z/ρ are indeed proportional to $\rho^{-1/2}$.

A reviewer of this paper drew the attention of the present author to a paper by Creager and Paris[17], where the stresses from eqns (15) and (18) together are already given in another notation. They are meant for the tip-region of an elliptical hole of great eccentricity or a notch in the shape of a slender hyperbola, thus in both cases for a parabolic region. They also give similar results for modes II and III (Sections 3.2 and 3.3).

3.2. *Mode II*

Stress functions (4) of the dominant eigenstate of the semi-infinite crack are

$$\phi[z] = -i\frac{K_{II}}{\sqrt{(2\pi)}} z^{1/2}, \qquad \psi[z] = \frac{3}{2} i \frac{K_{II}}{\sqrt{(2\pi)}} z^{1/2}. \tag{22}$$

The shear stress τ along the positive x-axis is

$$\tau = \frac{K_{II}}{\sqrt{(2\pi)}} x^{-1/2}. \tag{23}$$

In order that the tractions along parabola (17) disappear, to stress functions (27) must be added

$$\phi_a[z] = 0, \qquad \psi_a[z] = \mathrm{i}\frac{K_{\mathrm{II}}}{\sqrt{(2\pi)}} z\rho^{-1/2}. \tag{24}$$

A stress-rounding factor cannot be defined similar to that for mode I, because in the top of the parabola all stresses are now zero. This fact does not seem to be recognized in Ref. [3, p. 404(6)] where an erroneous formula is reported.

The maximum stress τ occurs at $x = 3\rho/2$, $y = 0$ (i.e. distance ρ from the top) and equals $\tau = 2K_{\mathrm{II}}\rho^{-1/2}/3\sqrt{(3\pi)}$, but the most severe stresses occur at the boundary in $x = 0$, $y = \pm\rho$ where the (tangential) normal stress σ attains its extreme values

$$\sigma_{\mathrm{extr}} = \mp\frac{K_{\mathrm{II}}}{\sqrt{\pi}}\rho^{-1/2} \tag{25}$$

The stress-rounding factor R_{II} is again the quotient of the coefficients of eqns (25) and (23)

$$R_{\mathrm{II}} = \sqrt{2}. \tag{26}$$

From eqns (23), (25) and (26)

$$|\sigma_{\mathrm{extr}}| = \frac{K_{\mathrm{II}}}{\sqrt{(2\pi)}} R_{\mathrm{II}}\rho^{-1/2}, \qquad (R_{\mathrm{II}} = \sqrt{2}). \tag{27}$$

3.3. *Mode III*

Stress function (11) of the dominant eigenstate is

$$\phi[z] = -2\frac{K_{\mathrm{III}}}{\sqrt{(2\pi)}} z^{1/2}. \tag{28}$$

The shear stress τ_y along the positive x-axis is

$$\tau_y = \frac{K_{\mathrm{III}}}{\sqrt{(2\pi)}} x^{-1/2}. \tag{29}$$

Remarkably the state of stress, eqn (28), leaves parabola (17) traction free and the maximum value of τ_y at the top of the parabola is

$$(\tau_y)_{\max} = \frac{K_{\mathrm{III}}}{\sqrt{\pi}}\rho^{-1/2}. \tag{30}$$

The stress-rounding factor R_{III} is the quotient of the coefficients of eqns (30) and (29)

$$R_{\mathrm{III}} = \sqrt{2} \tag{31}$$

and

$$(\tau_y)_{\max} = \frac{K_{\mathrm{III}}}{\sqrt{(2\pi)}} R_{\mathrm{III}}\rho^{-1/2}, \qquad (R_{\mathrm{III}} = \sqrt{2}). \tag{32}$$

This result occurs without proof in Ref. [3, p. 404(7)].

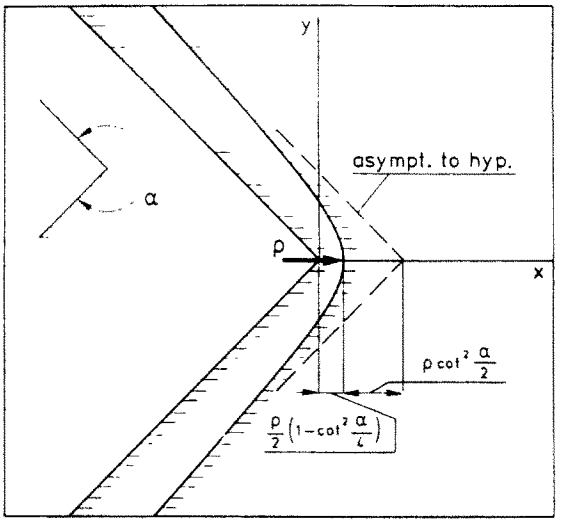

Fig. 2. The wedge-shaped region and the rounding. The top of the hyperbola is at $x = (\rho/2)(1 - \cot^2\alpha/4)$, but may be at an arbitrary point on the positive x-axis.

4. METHOD OF SOLUTION FOR WEDGE ANGLE $\pi < \alpha < 2\pi$

4.1. *Mode I*

The axis of symmetry of the infinite wedge-shaped region is the x-axis. The boundaries (situated in the left half-plane) are (Fig. 2)

$$y = \pm x \operatorname{tg}\frac{\alpha}{2}. \tag{33}$$

Stress functions (4) of the dominant eigenstate (of the non-rounded wedge) are

$$\phi[z] = \frac{K_I}{\sqrt{(2\pi)}} z^{\lambda+1} \frac{\sin\alpha}{A[\lambda]} \tag{34}$$

$$\psi[z] = \frac{K_I}{\sqrt{(2\pi)}} z^{\lambda+1} \frac{\sin(\lambda\alpha)}{A[\lambda]} \tag{35}$$

$$A[\lambda] = (\lambda^2 + 3\lambda + 2)\sin\alpha + (\lambda + 1)\sin(\lambda\alpha) \tag{36}$$

and λ is the smallest root > -1 of

$$\sin\{(\lambda + 1)\alpha\} + (\lambda + 1)\sin\alpha = 0. \tag{37}$$

The expression for $A[\lambda]$ is chosen such that along the positive x-axis the stress σ_y is

$$\sigma_y = \frac{K_I}{\sqrt{(2\pi)}} x^{\lambda} \tag{38}$$

and the coefficient K_I is defined as the stress-intensity factor of the stress singularity of the wedge. Note, however, that this stress-intensity factor has not the dimension of that of fracture mechanics.†

The rounding of the sharp corner is achieved by considering a new boundary in the

† In Ref. [6] is used $\sigma_y = (K_I/\sqrt{2})x^{\lambda}$. Compare footnote on p. 241.

wedge-shaped region close to its sides, eqn (33). This boundary is the left branch of a hyperbola (in the sequel with the notion hyperbola only this left branch is meant) with its asymptotes parallel to the wedge sides (Fig. 2)

$$z = \rho \frac{\cos(\alpha/2)}{\cos(\alpha/2) - \cos(\zeta\alpha/2)} e^{-i\zeta\alpha/2}, \qquad -1 < \zeta < 1 \tag{39}$$

and the hyperbola passes into parabola (17) for $\alpha = 2\pi$. The focus is in $z = 0$, the top in $z = \rho \cos(\alpha/2)/(\cos(\alpha/2) - 1) = (\rho/2)(1 - \cot^2 \alpha/4)$, the radius of curvature at the top is ρ. .

With stress functions (34), (35), expression (10) does not become constant along the new boundary now considered, but

$$\phi[t] + t\overline{\phi'[t]} + \overline{\psi(t)} = f[t]. \tag{40}$$

Additional stress functions $\phi_a[z]$ and $\psi_a[z]$ are necessary to make the new boundary traction free. Obviously the boundary condition for these stress functions is

$$\phi_a[t] + t\overline{\phi_a'[t]} + \overline{\psi_a[t]} = -f[t]. \tag{41}$$

The tractions to be removed and therefore also all the stresses of $\phi_a[z]$ and $\psi_a[z]$ tend to zero for $z \to \infty$ according to $|z|^{\lambda-1}$, whereas the stresses of eqns (34) and (35) generally only according to $|z|^{\lambda}$. Therefore, one need not fear that removal of the tractions from the new boundary leads only to vanishing stresses everywhere. Moreover, the tractions to be removed tend to zero strongly enough (stronger than $1/|z|$) to guarantee a unique solution for the stresses of $\phi_a[z]$ and $\psi_a[z]$. At related problems Neuber[12, pp. 166–174] uses instead of eqn (39) as a boundary another generalization of parabola (17), $z = c(1 - i\eta)^{\alpha/\pi}$ and c is a constant determined by the radius of curvature at the top on the x-axis. This curve resembles a hyperbola but it has no asymptotes and the tractions along this boundary tend too weakly to zero and no unique solutions for their interior stresses exist (the parabola of Section 3, though also without asymptotes, does allow a unique—and even exact—solution). Besides such a non-unique solution cannot be obtained along the numerical way, which one is enforced to follow, because some of the integrations which should be carried out will be divergent.

The procedure to obtain the solution for $\phi_a[z]$ and $\psi_a[z]$ from their tractions is described in Refs [9, pp. 408–412; 10, pp. 313–317]. The most important step is to solve a complex auxiliary function $\omega[t]$ from the integral equation

$$\omega[t] + \frac{1}{2\pi i}\int \omega[s]\, d \ln \frac{s - t}{\bar{s} - \bar{t}} - \frac{1}{2\pi i}\int \overline{\omega[s]}\, d \frac{s - t}{\bar{s} - \bar{t}} = -f[t]. \tag{42}$$

The integration variable s like t takes the z-values of the hyperbola and the integration extends all along the hyperbola in the direction of the positive y-values to negative y-values. The closing arc of angle α at infinity does not contribute.

By a suitable distribution of integration points the equation was solved numerically. The number of integration points was 320. To judge the accuracy sometimes also only 160 and 80 points were used.

The additional stress functions $\phi_a[z]$ and $\psi_a[z]$ and their derivatives are now for z in the region under consideration, but not on the boundary (the hyperbola)

$$\phi_a[z] = \frac{1}{2\pi i}\int \frac{\omega[t]}{t - z} dt \tag{43}$$

$$\phi_a'[z] = \frac{1}{2\pi i}\int \frac{\omega[t]}{(t - z)^2} dt \tag{44}$$

$$\phi_a''[z] = \frac{2}{2\pi i}\int \frac{\omega[t]}{(t-z)^3}\,dt \tag{45}$$

$$\psi_a[z] = \frac{1}{2\pi i}\int \frac{\overline{\omega[t]} - \bar{t}\omega'[t]}{t-z}\,dt \tag{46}$$

$$\psi_a'[z] = \frac{1}{2\pi i}\int \frac{\overline{\omega[t]} - \bar{t}\omega'[t]}{(t-z)^2}\,dt. \tag{47}$$

Again the integrals extend all along the hyperbola in the direction of positive y-values to negative y-values. If the point z is near the boundary the integrands behave badly. Then a point t_0 on the boundary is chosen in the neighbourhood of z. With the aid of computed derivatives $\omega'[t_0]$, $\omega''[t_0]$, etc. and a Taylor series an analytical continuation (only valid in the neighbourhood of t_0) $\omega[z]$ of $\omega[t]$ as well as derivatives $\omega'[z]$ and $\omega''[z]$ are determined.

To the right-hand side of eqn (43) are now added two terms which obviously are zero together

$$\phi_a[z] = \frac{1}{2\pi i}\int \frac{\omega[t]}{t-z}\,dt - \frac{\omega[z]}{2\pi i}\oint \frac{1}{t-z}\,dt + \omega[z]. \tag{48}$$

The second integral is along the hyperbola and closing arc at infinity, but when the second integral is taken only along the hyperbola, the last term is reduced to $(1 - \alpha/2\pi)\omega[z]$ and

$$\phi_a[z] = \frac{1}{2\pi i}\int \frac{\omega[t] - \omega[z]}{t-z}\,dt + \left(1 - \frac{\alpha}{2\pi}\right)\omega[z]. \tag{49}$$

The integrand now behaves smoothly, even if z is on the boundary. Then for $t = z$ the integrand is $\omega'[t]$. By the introduction of $\omega[z]$ into the integrand the integration is only convergent if the contributions at y and $-y$ are taken together, which is allowed. Besides numerically this is of course not necessary.

The smoothing of the integrands of eqns (44) and (45) leads to

$$\phi_a'[z] = \frac{1}{2\pi i}\int \left\{\frac{\omega[t] - \omega[z]}{(t-z)^2} - \frac{\omega'[z]}{t-z}\right\} dt + \left(1 - \frac{\alpha}{2\pi}\right)\omega'[z]. \tag{50}$$

For $t = z$ the integrand is $\omega''[t]/2$

$$\phi_a''[z] = \frac{2}{2\pi i}\int \left\{\frac{\omega[t] - \omega[z]}{(t-z)^3} - \frac{\omega'[z]}{(t-z)^2} - \frac{1}{2}\frac{\omega''[z]}{t-z}\right\} dt + \left(1 - \frac{\alpha}{2\pi}\right)\omega''[z]. \tag{51}$$

For $t = z$ the integrand is $\omega'''[t]/6$.

The same smoothing is carried out for eqns (46) and (47). The stress functions $\phi_a[z]$ and $\psi_a[z]$ are only computed for checking purposes. With the derivatives their stresses are computed with eqns (5) and (6). They must be added to the stresses of eqns (34) and (35).

A fair check on the calculations is of course the freedom of tractions on the boundary. Not only eqn (10) must be zero or at least constant but also eqn (7) must be zero there.

It can be proved that if the top of the hyberbola is shifted to another point $x > 0$, its final stress field is shifted unaltered too. This was indeed very fairly confirmed in a numerical experiment.

4.2. *Mode II*

The derivations for mode II are the same as those for mode I. Only eqns (34)–(38) are to be changed into

$$\phi[z] = \mathrm{i}\frac{K_{\mathrm{II}}}{\sqrt{(2\pi)}} z^{\lambda+1} \frac{\sin\alpha}{B[\lambda]} \tag{52}$$

$$\psi[z] = -\mathrm{i}\frac{K_{\mathrm{II}}}{\sqrt{(2\pi)}} z^{\lambda+1} \frac{\sin(\lambda\alpha)}{B[\lambda]} \tag{53}$$

$$B[\lambda] = (\lambda^2 + \lambda)\sin\alpha - (\lambda + 1)\sin(\lambda\alpha) \tag{54}$$

$$\sin\{(\lambda + 1)\alpha\} - (\lambda + 1)\sin\alpha = 0 \tag{55}$$

$$\tau = \frac{K_{\mathrm{II}}}{\sqrt{(2\pi)}} x^{\lambda}. \tag{56}$$

The wedge angle, however, does only vary from $\beta < \alpha < 2\pi$ and β is a solution of $\mathrm{tg}\,\beta = \beta$, $\beta = 257.4534°$. Below that α-value $\lambda > 0$ and there are no stress intensities and stress concentrations and calculations have no sense. Besides these calculations would be impossible because the tractions to be removed tend for $|z| \to \infty$ too weakly to zero.

4.3. *Mode III*

Stress function (11) for the dominant eigenstate (of the non-rounded wedge) is

$$\phi[z] = -\frac{K_{\mathrm{III}}}{\sqrt{(2\pi)}} \frac{z^{\lambda+1}}{\lambda + 1} \tag{57}$$

and λ is the smallest root of eqn (3) greater than -1, being $\lambda = \pi/\alpha - 1$. Along the positive x-axis

$$\tau_y = \frac{K_{\mathrm{III}}}{\sqrt{(2\pi)}} x^{\lambda} \tag{58}$$

and the coefficient K_{III} is defined as a stress-intensity factor.

Along the new boundary, eqn (39)

$$\phi[t] + \overline{\phi[t]} = f(t) \tag{59}$$

and in view of eqn (14) an additional $\phi_a[z]$ is necessary to remove these tractions and its boundary condition is

$$\phi_a[t] + \overline{\phi_a[t]} = 2\,\mathrm{Re}\,\phi_a[t] = -f(t). \tag{60}$$

The procedure to obtain the solution for $\phi_a[z]$ is described in Ref. [13, pp. 137, 138]. A real auxiliary function $\omega[t]$ must be solved from the integral equation

$$\omega[t] + \frac{1}{2\pi\mathrm{i}} \int \omega[s]\,\mathrm{d}\ln\frac{s - t}{\bar{s} - \bar{t}} = -f(t). \tag{61}$$

This integral equation is simpler than that of eqn (42), in the first place because in eqn (42) the function $\omega[t]$ is complex.

With

$$\phi_a[z] = \frac{1}{2\pi i}\int \frac{\omega[t]}{t-z}\mathrm{d}t \tag{62}$$

and eqns (12), (44) and (50) follow the shear stresses to be added to the shear stresses of eqn (57).

4.4. *Further possibility of testing the numerical procedures*

Apart from the checks on the rightness of the calculations (last two alineas Section 4.1) there is a further fair opportunity to judge the accuracy of all the numerical procedures which involve higher-order differentiation, integration and interpolation rules because an exact solution for mode III can be found. This was done by means of elliptic coordinates $u, v, z = \cosh w, w = u + iv$ and the stress-function $\phi[w] = i\cosh\{(\lambda + 1)w\}$. The real part of this function is zero on the left branch of the hyperbola $z = \cosh(u + i\alpha/2)$.

Exact solutions of this type for modes I and II are not possible, though exact plane strain and stress fields with the *two* branches of a hyperbola traction free are well known[12, pp. 39–47].

Neuber[12, pp. 167 and 168] obtains, for mode III only, an analytical solution which indeed satisfies exactly the partial differential equation and the condition for his boundary $z = c(1 - i\eta)^{\alpha/\pi}$. But as was explained (Section 4.1) such a solution is not unique. If his results are somewhat rearranged, there are differences of about 10% with present results.

5. NUMERICAL RESULTS

5.1. *Mode I*

As in Section 2.1 for the semi-infinite crack (wedge of angle $\alpha = 2\pi$), a stress-rounding factor R_I is defined by means of the stress-intensity factor K_I of eqn (38) and the maximum stress σ_y which occurs at the top of the hyperbola

$$(\sigma_y)_{max} = \frac{K_I}{\sqrt{(2\pi)}} R_I \rho^{\lambda}. \tag{63}$$

The values for λ and R_I are given in Table 1. Care is taken that generally also the last decimals given are correct.

Hahn[14, p. 14(29)] gives calculations for a square hole with rounded corners and estimates for the four $\alpha = 270°$ wedges a λ-value -0.5, but admittedly the difference with the proper value (-0.455516) is not very large. No antimetrical state of stress is present in Hahn's wedges. In that case the true λ-value differs strongly from -0.5 (Table 2(a)).

Table 1. Stress-rounding factors R_I

α (deg.)	λ of eqn (37)	R_I of eqn (63)
180	0	1
195	−0.142668	1.612758
210	−0.248025	1.992344
240	−0.384269	2.443757
270	−0.455516	2.665111
300	−0.487779	2.768503
330	−0.498547	2.8135
360	−0.5	$2\sqrt{2}$

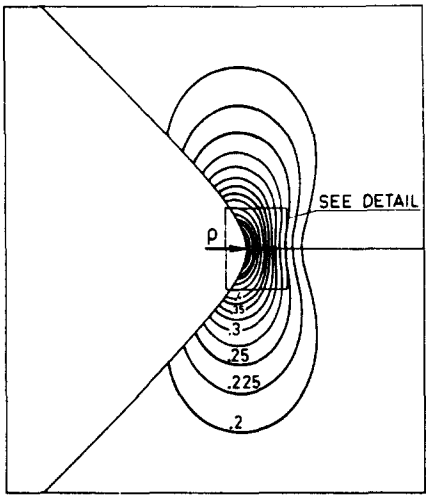

Fig. 3. Mode I. Lines of equal dimensionless Von Mises effective stress $\sigma_e/K_I\rho^\lambda$. Poisson's ratio 0.3, wedge angle $\alpha = 270°$, $\lambda = -0.4555$.

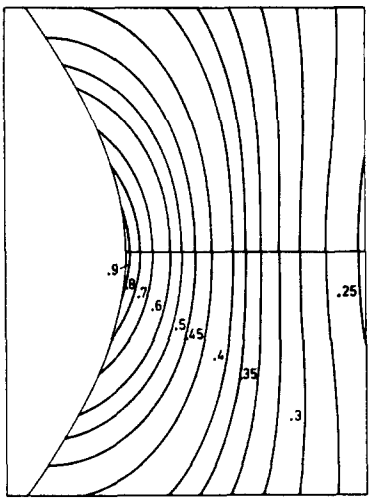

Fig. 4. Detail of Fig. 3 (measure of figure $(3/2)\rho \times 2\rho$).

Figure 3 (detail Fig. 4) shows within the region of the rounded wedge of angle $\alpha = 270°$ lines of equal Von Mises effective stress σ_e for plane strain ($\nu = 0.3$) computed with the formula

$$\sigma_e^2 = \sigma_x^2 + \sigma_y^2 + \sigma_3^2 - \sigma_y\sigma_3 - \sigma_3\sigma_x - \sigma_x\sigma_y + 3\tau^2 \tag{64}$$

and with eqn (9)

$$\sigma_e^2 = (\sigma_x^2 + \sigma_y^2)(1 - \nu + \nu^2) - \sigma_x\sigma_y(1 + 2\nu - 2\nu^2) + 3\tau^2. \tag{65}$$

In Ref. [15] many similar graphs will be given also for other angles α, for modes II and III and for plane stress, i.e. $\nu = 0$.

5.2. *Mode II*

For mode II the stress-rounding factor is defined by means of the extreme values of the tangential normal stress which occur on two places at the boundary

$$|\sigma_{extr}| = \frac{K_{II}}{\sqrt{(2\pi)}} R_{II}\,\rho^\lambda. \tag{66}$$

Table 2(a) gives values of R_{II} and the coordinates of the points on the boundary of these

Table 2(a). Stress-rounding factors R_{II} (the x' coordinate from the top of the hyperbola)

α (deg.)	λ of eqn (55)	R_{II} of eqn (66)	Coord. of place $\pm\lvert\sigma_{extr}\rvert$ x'/ρ	$\mp y/\rho$
257.4534	0	1.666844	−0.669	1.426
260	−0.019525	1.674068	−0.581	1.281
270	−0.091471	1.715070	−0.469	1.076
300	−0.269099	1.803234	−0.446	0.979
330	−0.401808	1.7567	−0.480	0.988
360	−0.5	$\sqrt{2}$	−0.5	1

Table 2(b). τ_{max} (at $y = 0$, x' from the top of the hyperbola)

α (deg.)	λ of eqn (55)	$\frac{\sqrt{(2\pi)}\tau_{max}}{K_{II}\rho^{\lambda}}$	x'/ρ of place τ_{max}
257.4534	0	1	∞
260	−0.019525	0.954819	5.83
270	−0.091471	0.877002	2.184
300	−0.269099	0.776696	1.208
330	−0.401808	0.695245	1.038
360	−0.5	$2\sqrt{2}/3\sqrt{3}$	1

extrema. The x' coordinate has its origin at the top of the hyperbola, $x - x' = \frac{1}{2}(1 - \cot^2\alpha/4)\rho$.

Along the x-axis the shear stress τ attains its maximum value, but its effective Von Mises stress is less than that of the reported σ_{extr} of Table 2(a). Only for $\alpha < 259°$ ($\nu = 0$) or $\alpha < 268°$ ($\nu = 0.3$) is this effective stress larger than that of σ_{extr}. But if λ approaches zero there is hardly any stress concentration at all. Table 2(b) gives this shear stress in dimensionless form $\sqrt{(2\pi)}\tau_{max}/K_{II}\rho^{\lambda}$. Compare these values with R_{II} of Table 2(a).

Figures 5 and 6 give lines of equal effective stress ($\nu = 0.3$) for $\alpha = 270°$.

5.3. *Mode III*

The maximum shear stress τ_y occurs at the top of the hyperbola

$$(\tau_y)_{max} = \frac{K_{III}}{\sqrt{(2\pi)}} R_{III}\rho^{\lambda}. \tag{67}$$

Table 3 gives values of the stress-rounding factor R_{III}.

The values of R_{III} agree with the exact values (Section 4.4)

$$R_{III} = \left(\sin\frac{\alpha}{2}\right)^{1-2\pi/\alpha}\left(-\frac{1}{2}\cos\frac{\alpha}{2}\right)^{\pi/\alpha - 1}. \tag{68}$$

Figure 7 gives lines of equal effective stress.

5.4. *Change of shape of the rounding*

Of course in practice the rounding of a sharp corner will generally not have exactly a hyperbolic shape. The present use of hyperbolas is the obvious generalization of the well-accepted use of the parabolic boundary for a rounded incision or crack ($\alpha = 360°$).

Other smooth curves with the same radius at the top and the same directions of the asymptotes as those of the hyperbola, or circular arc with tangents in the proper directions, will not differ very much from the hyperbolas used. The exponents λ are not affected at all and the influence on the stress-rounding factors is only very small.

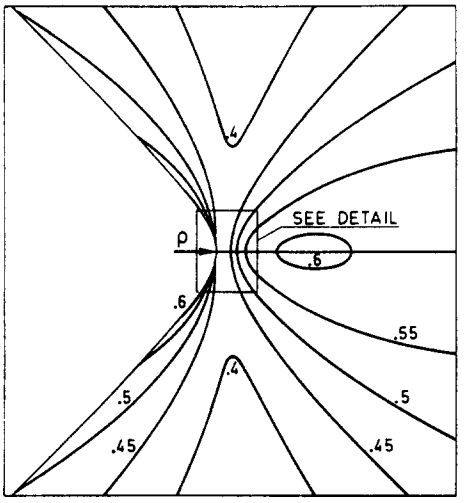

Fig. 5. Mode II. Lines of equal dimensionless Von Mises effective stress $\sigma_e/K_{II}\rho^{\lambda}$. Poisson's ratio 0.3, wedge angle $\alpha = 270°$, $\lambda = -0.0915$.

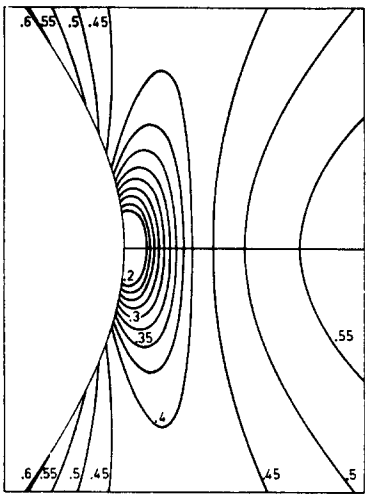

Fig. 6. Detail of Fig. 5 (measure of figure $(3/2)\rho \times 2\rho$).

Table 3. Stress-rounding factors R_{III}

α (deg.)	$\lambda = \frac{\pi}{\alpha} - 1$	R_{III} of eqn (67)
180	0	1
195	−0.076923	1.242616
210	−0.142857	1.372829
240	−0.25	1.519671
270	−0.333333	1.587401
300	−0.4	1.605483
330	−0.454545	1.57413
360	−0.5	$\sqrt{2}$

As a test case is tried for mode III (where exact solutions are possible) and $\alpha = 270°$, another boundary[16, pp. 46 and 47]

$$9(z/\rho)^{4/3} - 16(z/\rho)^{1/3} + 9\eta = 0$$

$$\eta_0 < \eta < \infty, \qquad \eta_0 = 3(4/9)^{4/3}. \tag{69}$$

This boundary has its top in $z = 4\rho/9$, asymptotes in the proper directions $y = \mp x \operatorname{tg} 135°$ and the radius in the top is ρ. At a distance 2ρ from the top it has y-values 0.0549ρ smaller than those of the hyperbola.

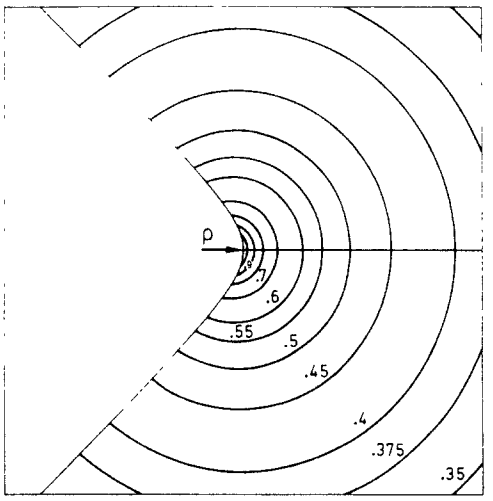

Fig. 7. Mode III. Lines of equal dimensionless Von Mises effective stress $\sigma_e/K_{III}\rho^{\lambda}$. Wedge angle $\alpha = 270°$, $\lambda = -1/3$.

The solution for the stress function $\phi[z]$ of eqn (11) is

$$\phi[z] = -\frac{K_{III}}{2\sqrt{(2\pi)}}(9z^{4/3} - 16\rho z^{1/3} + 9\rho^{4/3}\eta_0)^{1/2}. \tag{70}$$

The stress-rounding factor becomes

$$R_{III} = (3/2)^{7/6} = 1.604870$$

and this is only 1.1% more than the value of Table 3 (1.587401).

Acknowledgement—The author gratefully acknowledges Th. Douma for his work in constructing the extensive computer programs.

REFERENCES

1. M. L. Williams, Surface stress singularities resulting from various boundary conditions of plates in extension. *J. Appl. Mech.* **19**, 526 (1952).
2. R. D. Gregory, Green's functions, bi-linear forms, and completeness of the eigenfunctions for the elastostatic strip and wedge. *J. Elasticity* **9**, 283 (1979).
3. D. P. Rooke, F. I. Baratta and D. J. Cartwright, Simple methods of determining stress intensity factors. *Engng Fracture Mech.* **14**, 397 (1981).
4. H. Tada, P. C. Paris and G. R. Irwin, *The Stress Analysis of Cracks Handbook*. Del Research Corp., St. Louis (1973).
5. F. Erdogan, Stress-intensity factors. *J. Appl. Mech.* **50**(50th Ann. Vol.), 992 (1983).
6. D. M. Tracy and T. S. Cook, Analysis of power type singularities using finite elements. *Int. J. Num. Meth. Engng* **11**, 1225 (1977).
7. K. Y. Lin and P. Tong, Singular finite elements for the fracture analysis of V-notched plate. *Int. J. Num. Meth. Engng* **15**, 1343 (1980).
8. G. H. Staab, A variable power singular element for analysis of fracture mechanics problems. *Comput. Struct.* **17**, 449 (1983).
9. N. I. Muskhelishvili, *Some Basic Problems of the Mathematical Theory of Elasticity*. Noordhoff, Groningen (1953).
10. I. S. Sokolnikoff, *Mathematical Theory of Elasticity*. McGraw-Hill, New York (1956).
11. G. R. Irwin, *Fracture*. Handbuch der Physik (Herausgegeben von S. Flügge), Band VI, *Elastizität und Plastizität*, p. 551 (1958).
12. H. Neuber, *Kerbspannungslehre*. Springer, Berlin (1958).
13. S. G. Mikhlin, *Integral Equations*. Pergamon Press, London (1957).
14. H. G. Hahn, Uber den Einfluss des Flankenwinkels auf die Spannungserhöhung an Kerben. *Acta Mech.* **1**, 1 (1965).
15. J. P. Benthem and Th. Douma, Graphs of the state of stress at rounded corners. Report to be published.
16. H. Kober, *Dictionary of Conformal Representations*. Dover, New York (1952).
17. M. Creager and P. C. Paris, Elastic field equations for blunt cracks with reference to stress corrosion cracking. *Int. J. Fracture Mech.* **3**, 247 (1967).